A&A 384, 702–710 (2002)
DOI: 10.1051/0004-6361:20020023

Astronomy & Astrophysics

Spectrophotometry and structural analysis of 5 comets⋆

Gy. M. Szabó[1], L. L. Kiss[1], K. Sárneczky[2], and K. Sziládi[1]

[1] Department of Experimental Physics & Astronomical Observatory, University of Szeged, 6720 Szeged, Dóm tér 9., Hungary
[2] Department of Physical Geography, ELTE University, 1088 Budapest, Ludovika tér 2., Hungary

Received 2 November 2001 / Accepted 4 January 2002

Abstract. We discuss the morphology and spectrophotometry of 5 comets visible in August, 2001. We decompose comae into coma profiles and azimuthally renormalized images, in which general and local features are quantitatively comparable. Comet 19P/Borrelly showed a strong gas fan toward the solar direction, but no detectable gas in the tail. Dust in its inner coma was collimated toward the antisolar direction and the tail, with no dust in the outer coma. The contribution of spatial variations structure was moderate, about 35%. Comet 29P/Schwassmann-Wachmann 1 was observed in outburst: we detected "spinning" jet structures. A high level of dust production resulted in an unusually high $Af\rho = 16\,600$ cm. The spatial variations reached −77%, at the minimum, due in part to a jet and a ring-like structure in 1 arcmin distance from the nucleus. In comet C/2001 A2, we detected a strong post-perihelion increase of dust and gas activity, in which the C_2 profile became one magnitude brighter over a 3-day period. For comets C/2000 SV74 and C/2000 WM1, we present detailed pre-perihelion spectrophotometry and morphological information. Comet C/2000 SV74 showed high dust production ($Af\rho = 1479$ cm). Its coma suggests a steady-state outflow of material, while the low contribution of spatial variations support high level activity. The coma of C/2000 WM1 is dominated by solar effects, and CO+ forms the bulk of its gas activity. Despite its large heliocentric distance, we observed a nice tail.

Key words. solar system: general – comets: individual: 19P/Borrelly, 29P/Schwassmann-Wachmann 1, C/2000 SV74 (LINEAR), C/2000 WM1 (LINEAR), C/2001 A2 (LINEAR)

1. Introduction

The distribution of distinctive cometary components (dust, ions, radicals) can be well studied with help of two-dimensional, narrow-band CCD images. In addition to measuring the spatial distribution of species, one can measure column densities of gas and dust, and draw conclusions on chemical composition, production rates and activity levels. Despite the efficiency of this method, only a small fraction of visible comets are studied with detailed spectrophotometry. Spectroscopic methods, on the other hand, have the advantage of producing a spectrum with a well-defined continuum level, so emission features show clearly. Large spectrophotometric and spectroscopic surveys of many comets were published by A'Hearn et al. (1995) (hereafter A95) and Fink & Hicks (1996), where the interested reader can find detailed descriptions of methods.

Surface photometry of images can address coma morphology (such as radial coma profiles and non-radial features, also called coma profiles and azimuthally renormalized images, see, e.g., Lederer et al. 1997; Larson & Slaughter 1991), and also may yield estimated nuclear radii (e.g. Luu & Jewitt 1992; Lamy & Tóth 1995; Lowry et al. 1999). An appropriate selection of medium- and narrow-band filters centered on different wavelengths can separate the dust continuum from emission by gas. Differences in gas and dust components reveal the effect of radiation pressure on different types of particles (a good example of combined quantitative coma analysis can be found, e.g. in Schulz et al. 1993).

The main aim of our work is to contribute to this field of ground-based solar system research with new narrow- and medium-band spectrophotometric observations of comets visible in August, 2001. The function of this paper is to present the results of observations of 5 comets carried out at Calar Alto Observatory. The paper is organised as follows. Section 2 deals with the observations, methods of analysis are described in Sect. 3, results on individual objects are given in Sect. 4, while the discussion is presented in Sect. 5. This work is an extension of our previous analysis of distant active comets (Szabó et al. 2001).

Send offprint requests to: L. L. Kiss,
e-mail: l.kiss@physx.u-szeged.hu

⋆ Based on observations taken at the German-Spanish Astronomical Centre, Calar Alto, operated by the Max-Planck-Institute for Astronomy, Heidelberg, jointly with the Spanish National Commission for Astronomy.

Table 1. Filter characteristics. Band is shown in nm/nm, filter diameter D in mm.

Filter	Band	Transm.	D(mm)	Code
Comet CN	387.1/5.0	35%	42	CN
Gunn v	411.1/37.4	19%	50	v
Comet CO+	425.4/6.9	56%	32	CO+
Gunn g	492.5/54.0	74%	50	g
Comet C_2	512.5/12.5	65%	42	C_2
Gunn r	662.6/104.5	77%	50	r
753/30	751.5/28.2	57%	50	j
Gunn z	910.0/90.0	90%	50	z

2. Observing strategy and data acquisition

Our primary goal was to obtain spectrophotometric observations that would enable morphological as well as quantitative studies of bright and moderately bright comets. The most important constraints were: 1) to separate comet continuum and emission bands and 2) to record the detected signal at the high S/N level required for detailed morphological calculations. The first required that the selected photometric system could exclude strong emission bands, while the second point required the use of medium- or wide-band photometry.

When selecting the filters, the main aim was to use medium-band filters to measure the continuum in the optical range up to 1 μ. The wide-band Johnson $BVRI$ system is not well-suited for this kind of work because it includes strong emission features in cometary spectra. Furthermore, the overlaps between the Johnson filters reduce their ability to trace continuum variations. Therefore, we decided to use the Gunn v, g, r, z filter sequence (Thuan & Gunn 1976), which is used mostly by extragalactic researchers. For quantitative spectrophotometry, we added interference filters: CN, CO+ and C_2 (see Table 1). As the wide-band standard Gunn i filter (Wade et al. 1979) passes the band of CN (2–0), we replaced it by an interference filter 753/30, similar in effective wavelength, which refer to as j in the tables. The Gunn z filter includes the 1 μm border of the continuum, and it also passes the CN (1–0) resonance line. Two of the interference filters, CN and CO+, just border the band of Gunn v. The Gunn g filter includes 70 percent of the C_2 filter band, which must be taken into account in reductions. Gunn r includes the $NH_2(0,10,0)$ band, which is not too strong even in the most active comets and does not influence the continuum flux significantly. A further advantage is that these filters avoid emission lines of airglow and light pollution, and so the background is significantly darker than it would be with Johnson filters. Table 1 summarizes the filter characteristics as given by the manufacturer. In Fig. 1, we compare our passbands to a typical model comet spectrum (Lowry et al. 1999; Arpigny 1995).

The observations were obtained at Calar Alto Observatory, with the 1.23 meter telescope equipped with a SITE#2b CCD camera on five nights in August, 2001. The image scale of the unbinned frames is 0.49″/pixel.

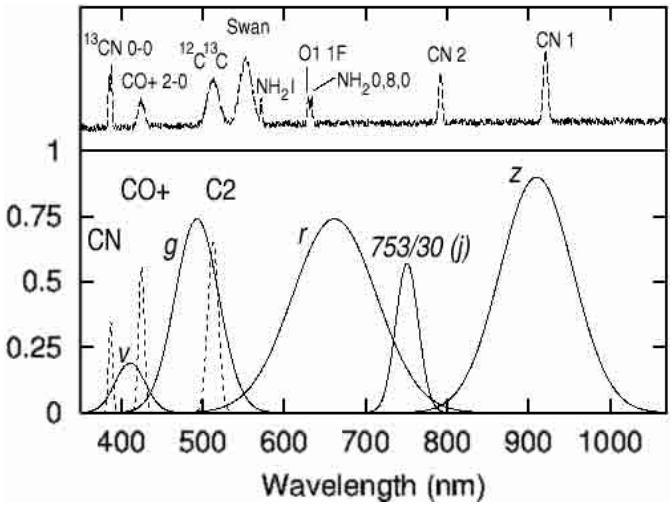

Fig. 1. Filter curves of our filters compared to a model spectrum of a comet showing most of the characteristic emission features. Italic labelled solid lines show the Gunn filters (simplified curves) and the 753/30 interference filter (referred as j in this paper), while dashed lines pertain to our special comet filters.

In order to avoid effects of image trailing, the telescope was set to follow the motion of the comets, not the ordinary sidereal rate. We chose comets predicted to be brighter than $r = 15\overset{\text{m}}{.}0$ (19P/Borrelly, 29P/Schwassmann-Wachmann 1, C/2000 SV74 LINEAR, C/2000 WM1 LINEAR, C/2001 A2 LINEAR) as targets. Their aspect data are summarized in Table 2. The full observing log is presented in Table 3.

The atmospheric extinction in the Gunn-system was monitored by repeated observations of BD+17°4708 selected from the lists of Thuan & Gunn (1976). The standard photometric transformations were determined by observations of Gunn-standards in the field of M 34 (Kent 1985) several times per night. Typical photometric uncertainties were $\pm 0\overset{\text{m}}{.}015$ in the extinction determination and $\pm 0\overset{\text{m}}{.}015$ in the zero-points of standard transformations. The overall uncertainty is estimated to be $\pm 0\overset{\text{m}}{.}022$–$0\overset{\text{m}}{.}033$, depending on the wavelength and target brightness. Two additional spectrophotometric standard stars (HD 187811 and HD 183439A) selected from Alekseeva et al. (1996) were also observed on Aug. 13, 2001 (MJD 52135.4).

3. Analysis and data reduction

The data obtained through the interference filters were calibrated following the usual methods of reduction as defined by A'Hearn (1983). Briefly, field stars on the same frames were measured with the narrow-band comet filters to find their $m_{\text{instr.}}$ instrumental magnitudes. These values were combined with the standard Gunn magnitudes and color indices in a least-squares fit to yield the color coefficients and stellar zero-points (κ_{XX}). For a given comet, the same coefficients and zero-points were used to determine expected narrow-band magnitudes, assuming that light is produced only by the comet's continuum.

Table 2. Aspect data of comets referred to the middle of the observing run. Signs used are: MJD modified Julian-Date, Δ geocentric radius, R heliocentric radius, ϵ elongation, α solar phase, Σ solar direction position angle μ_r sky brightness through Gunn r filter, See. seeing. MJD 52134.5 = 13th August, 2001, 0:00 UT.

Comet	MJD	Δ(AU)	R(AU)	ϵ	α	Σ	μ_r	See.	Airmass	Scale (km/″)	Code
19P/Borrelly	52137.66	1.685	1.400	56.8	36.4	87.6	20.3	2.2	2.9–1.9	1225	19P
29P/SW1	52135.35	5.121	5.919	138.6	6.5	294.8	20.4	1.4	2.4–2.6	3724	29P
C/2000 SV74	52135.53	4.036	4.244	93.3	13.8	102.0	20.7	1.0	1.6–1.4	2934	SV74
C/2000 WM1	52137.55	2.891	2.789	74.1	20.4	115.4	20.9	1.1	2.0–1.7	2102	WM1
C/2001 A2	52134.51	0.714	1.628	140.4	23.4	357.7	20	1.0	1.1	519	A2a
C/2001 A2	52136.50	0.747	1.655	139.8	23.2	357.6	20	1.1	1.4	543	A2b
C/2001 A2	52137.52	0.764	1.669	139.5	23.2	357.6	20.9	1.1	1.1	555	A2c

Table 3. Log of the individual images. Exp. means integrated exposure time in *"number of images"* × *"exposure time of one individual"* format. Remarks are: (1): has not been detected, or has been not brighter than about one fourth of the background scatter on the individual images. (2): effect of clouds is visible on images of the third sequence.

Code	Filter	Exp.(s)	Remark
19P	v, g, j	3 × 60	
	r, z, CO+, C_2, CN	6 × 60	
29P	v, g, r, j, z, CN, CO+, C_2	3 × 240	
SV74	v, g, r, j, z, C_2	3 × 120	
	CO+, CN	1 × 120	(1)
WM1	v, g, r, j, z, C_2	3 × 90	
	CN, CO+	1 × 90	(1)
A2a	g, r, C_2, CO+, CN	3 × 60	
A2b	r, v, g, j, z, CN, CO+, C_2	2 × 90	(2)
A2c	v, g, r, j, z, CN, C_2	3 × 105	
	CO+	1 × 120	(1)

Then the difference of the observed and expected narrow-band magnitudes is assigned to the emission bands. The resulting equations are:

$$m_{\rm instr.}^{\rm CN,stellar} = v + 0\overset{\rm m}{.}43(v-g) + \kappa_{\rm CN}$$
$$m_{\rm instr.}^{\rm CO+,stellar} = v - 0\overset{\rm m}{.}15(v-g) + \kappa_{\rm CO}$$
$$m_{\rm instr.}^{\rm C_2,stellar} = g - 0\overset{\rm m}{.}09(v-g) + \kappa_{\rm C_2}.$$

The κ zero points vary slightly, depending on sky conditions: roughly $2\overset{\rm m}{.}2$ for CN and CO+ and $1\overset{\rm m}{.}5$ for C_2; rms scatter of the fits to field stars is smaller than $0\overset{\rm m}{.}04$.

Having separated the emission and continuum, we calculated absolute fluxes of emission features based on observations of spectrophotometric standards HD 183439A and HD 187811 (Alekseeva et al. 1996). We determined flux excesses $F_{\rm CN}$, $F_{\rm CO+}$, $F_{\rm C_2}$; $F_{\rm XX} = F_{\rm XX,observed} - F_{\rm XX,stellar}$. For calculating the total luminosity, we assumed isotropic radiation from the coma: $L({\rm total}) = L({\rm measured}) \cdot 4\pi\Delta^2(m^2)$.

To describe dust continuum production, we adopted the $Af\rho$ values from A'Hearn (1983). The ρ radius was chosen by selecting the linear part of the surface brightness profile. The calculation also includes the flux ratio of the comet to the Sun. We needed the Gunn r magnitude of the Sun, which was calculated from the Johnson $R_\odot = -27\overset{\rm m}{.}26$ transformed to Gunn r according to the formula of Jørgensen (1996) $r - R = 0\overset{\rm m}{.}354$, rms = $0\overset{\rm m}{.}035$, resulting $r_\odot = -26\overset{\rm m}{.}91$. Gas production parameters describe the number of radicals ejected from the nucleus during one second. The fluorescence efficiencies (g-factors) and scale lengths were taken from A95 for CN and C_2 and from Cochran et al. (2000) for CO+.

To our knowledge, there are no precise Gunn colors of the Sun in the literature. However, we needed them to study the comet continuum reflectance, where spectral variations of the Sun have to be taken into account. Therefore, we measured precise colors of several main-belt asteroids with previously published medium-resolution optical spectra during our observing run. The best target was 2 Pallas, which has a largely constant reflectance spectrum over the visible wavelength (Gaffey et al. 1993), making it easy to transform its Gunn-colors to those of the Sun. Without giving the details (Szabó et al. 2002, in prep.) we estimate the following values: $(v\text{–}g)_\odot = 0.254$, $(g\text{–}r)_\odot = 0.126$, $(r\text{–}j)_\odot = 0.006$, $(j\text{–}z)_\odot = -0.009$, with photometric errors about $\pm 0\overset{\rm m}{.}02$.

As usual in morphological studies, field stars had to be subtracted from the comae. This was done with the DAOPHOT package in IRAF. For correct subtraction in the coma the foreground coma contribution was estimated based on manual examination of the coma, near the individual stars. The pixel intensities were modified that the background is zero and the integrated flux is 1. That allowed to isolate the coma contribution by a median combination of these star-subtracted images.

Further examinations were based on some tools commonly used in, e.g., galaxy morphology (see e.g. Ravindranath et al. 2001 for recent discussion). To extract the surface brightness change across the nucleus, we used the *apextract* task from the TWODSPEC package in IRAF. A 5.″0-wide aperture was shifted through the coma across the nucleus in two sampling directions. One of them was the solar-antisolar line (hereafter referred as radial section), the other perpendicular to the radial direction (hereafter referred as tangential section). *Azimuthally renormalized images* are similar to the residual images defined by the difference of the coma image and an analytic radial profile. But instead of an analytic fit, we simply used the radial coma image resulting from an azimuthally

averaged coma image. "Bright", positive areas in the residual image refer to matter excess while "dark", negative values show tenuous areas. This method emphasizes the presentation of special phenomena, such as the ellipticity of the coma, jet or spin structures. To describe these features, we extracted surface brightness profiles from the residual images, just as we did for the original images.

For physical conclusions, the strength of spatial variations must be characterized. We calculated *local intensity ratios* for the negative and positive peaks of azimuthally renormalized images. They are given by the peak intensities with respect to the normalised coma intensity at the same position.

4. Results

Absolute photometric data and calculated production parameters of comets are compared in Table 4. Values of r magnitude and color indices are measured in apertures of $10''$ radius, as well as the L total fluxes of emission features. They are followed by ρ [10^7 cm] radii, *slope* of the coma profile inside ρ radius and $Af\rho$ values measured inside ρ.

Remarks on the individual comets are as follows.

19P/Borrelly
This comet belongs to the Jupiter family, with an orbital period of about 7 years. It is the prototype of the Borrelly-type class of comets (defined by Fink et al. 1999), known for its low C_2 production. The 1994 perihelion was studied by A95, who determined several production rates. A detailed structural analysis of its coma and nucleus is presented by Lamy et al. (1998) based on observations taken during the same apparition. They have determined a prolate spheroid nucleus model with 4.4×1.8 km semi-axes. The estimated fractional active area is 8%. Our observations were made about two months before the Deep Space-1 spacecraft encountered this comet in September, 2001.

Images at relative high airmasses and under pretwilight conditions were taken because of the unfavorable elongation. The night of the best transparency conditions was selected for observations, although the seeing was larger than $2''$.

Although the slope of the profile (-0.98) suggests an isotropic and steady-state coma, the inner structure was quite complex. The nucleus was far from the coma center, shifted to the antisolar direction. Dust components formed a compact cloud in the inner $30''$ of the coma and formed an impressive tail with forked structure. Gas components flowed to the solar direction, with almost no gas observed in the tail. Surface photometry showed that the surface brightness of the inner coma decreased faster in the antisolar direction (2 magnitudes in $7''.5$ on the r images) and slower toward the Sun (2 magnitudes in $11''$). The outer coma became quite regular: it faded by 5 magnitudes in $53''$ to the antisolar direction and $37''$ to the solar one.

As the azimuthally renormalized image shows, the behavior of the inner coma is due to a jet-like outflow to the antisolar direction containing 16% of the total flux. This feature is detectable through $45''$ on the radial cross section, which implies a proper length of 65×10^3 km on the assumption that the jet is thin and lies on the solar radius. A comparison between the Gunn r and Comet C_2 profiles suggests that it consists solely of gaseous components. The tail is quite long and could be detected even beyond the border of the image. Within a $125''$ distance to the nucleus, it is brighter than 24 mag/arcsec^2. Images and profiles are presented in Fig. 2/19P.

29P/Schwassmann–Wachmann 1
This unusual comet is well-known for its unpredictable outbursts (see Enzian et al. 1997 and references therein). The nucleus seems to be perhaps the largest one known in the Solar System, while its albedo is often estimated to be over 15% – much higher than is measured for "usual" nuclei (Jewitt 1990). Jets of the comet in outburst suggest rotational effects. Several observers have tried to determine the rotation period: the most recently published values are 14 and 32 hours (Meech et al. 1993).

We observed the comet during its 2001 outburst, which was detected by Nakamura et al. (2001) on May 17.69, 2001. During our observations and reductions, the main difficulty was the crowded sky-field in the Milky Way. Our star-substraction procedure removed about 3500 stars brighter than about 21 magnitudes from the $10' \times 10'$ field.

Three months after the outburst the comet was $12^{\rm m}.68$ in Gunn r, thanks to its position at opposition and high activity. Due to the distance to the Earth, its coma was quite compact: its surface brightness decreased 2 magnitudes in $16''$ and 5 magnitudes in $35''$. The latter value corresponds to a diameter of 260×10^3 km. On the azimuthally renormalized images, the well-known jet shows a spiral-like matter-rich and matter-poor part, with local contributions +37% and −77%, respectively. The spinning shape is attributed to rotation of the nucleus.

A ring-like structure, also visible with help of surface photometry, is not included in the non-radial part as it vanishes by subtracting the azimuthal average from the coma image. The jet ends at $21''$, while this faint ring is suspected to be at $1'$ distance from the nucleus, having 22 mag/arcsec^2 surface brightness. Images are presented on the right side of Fig. 2/29P.

We believe that the low counts in CN, CO+ and C_2 filters originate from the continuum, and considering the estimated errors, only higher limits of the emission rates are reported.

C/2000 SV74 (LINEAR)
The comet, which reaches its perihelion on April 30.4, 2002, was observed in order to monitor the pre-perihelion activity. At a solar distance of 4.244 AU, the measured brightness of $15^{\rm m}.29$ suggests that it will be quite bright near perihelion.

Table 4. Magnitudes, colors and production parameters. L fluxes in 10^{15} erg s^{-1}, ρ in 10^7 cm and $Af\rho$ in cm.

Ref.	r	$v-g$	$g-r$	$r-j$	$j-z$	$L_{\rm CN}$	$L_{\rm C_2}$
19P	12.27	−0.07	0.26	−0.04	0.19	2150	531
29P	12.68	0.33	−0.07	0.32	0.01	<234	<593
SV74	15.29	0.22	0.58	0.22	0.02	<23	132
WM1	15.19	0.13	0.28	0.33	−0.15	<70	63
A2a	13.52	–	−0.06	–	–	126	57
A2c	13.46	−0.10	−0.11	0.11	0.15	830	274
Ref.	$L_{\rm CO+}$	ρ	slope	log $Af\rho$	[C$_2$]–[CN][a]	$[Af\rho]$–[C$_2$]	$[Af\rho]$–[CN]
19P	<52	60.5	−0.97	2.98	−0.38	−22.32	−22.70
29P	<329	148.0	−1.60	4.22	–	>−21.10	>−20.50
SV74	209	146.0	−1.21	3.17	>0.6	−21.12	>−20.52
WM1	396	105.0	−1.42	2.72	>0.2	−21.99	>−21.80
A2a	<4	22.5	−1.04	2.21	−0.12	−22.07	−22.19
A2c	<4	27	−1.07	2.28	−0.26	−22.74	−23.00

[a] Using log(Q(C$_2$)/Q(CN)), log($Af\rho$/Q(C$_2$)), log($Af\rho$/Q(CN)), production rates in mol s^{-1}, $Af\rho$ in cm.

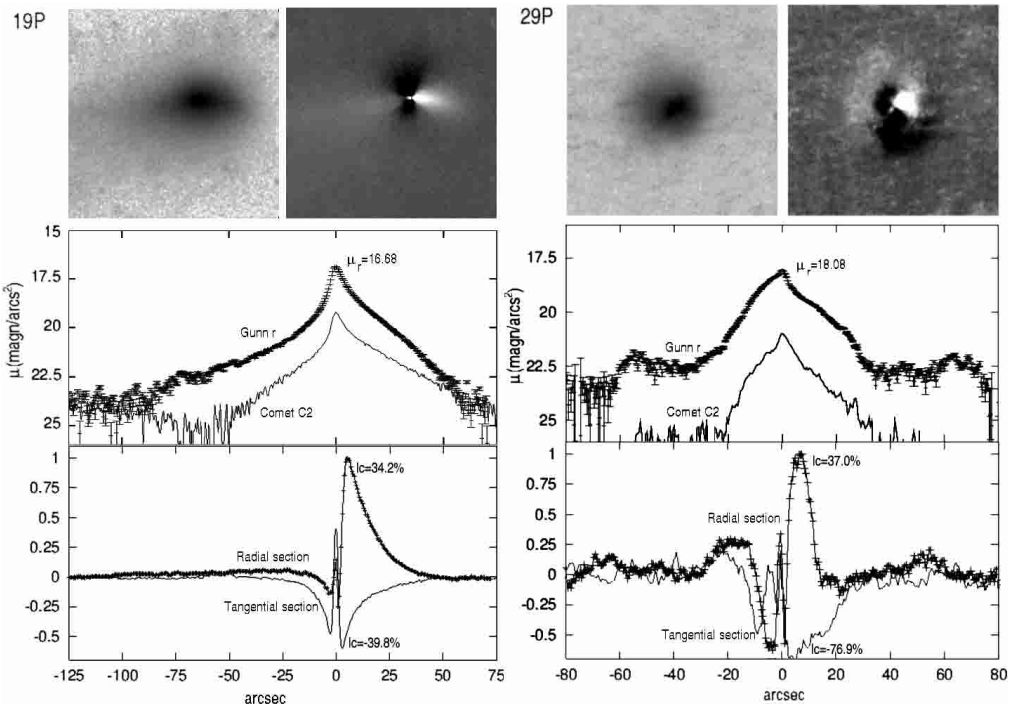

Fig. 2. Comets 19P (left) and 29P (right). The images are rotated in a such way the solar direction is to the right. The left subpanels show the observed images, while the right subpanels are azimuthally renormalized images. Graphs show radial sections of surface brightness profiles (middle) in standard Gunn r and C$_2$. C$_2$ is plotted with respect to the zero magnitude of Gunn g. Normalized intensity of spatial variations is shown in the bottom. Local intensity ratio (lc) of spatial variations is expressed in percents at positive and negative peaks. Crosses refer to the radial section while solid line shows the tangential section. The images are 150″×150″ for 19P and 100″×100″ for 29P.

We measure a decrease in surface brightness of 5 magnitude at 39″ (114×10^3 km) and 32″ on the solar and antisolar sides, respectively. No tail brighter than 24 mag/arcsec^2 was detected. The contribution of spatial variations was 33% at the maximum of the non-radial map and −22% at the minimum. The simple structure of spatial structure is explained by a regular isotropic surface activity in the presence of solar wind and radiation pressure. The slope of the coma profile is −1.21, which seems to be shallower than profiles at larger solar distances (see e.g. Szabó et al. 2001). The feature could be explained by strong and steady-state activity, containing mainly dust components. This assumption of dust activity is also consistent with the high $Af\rho$ (1892 cm) and the reddish color indices. We detected weak emission in C$_2$ and CO+.

C/2000 WM1 (LINEAR)

The comet was observed 5 months before its perihelion date of January 22.68, 2002. A compact circular coma was detected with a diameter of ∼20″.

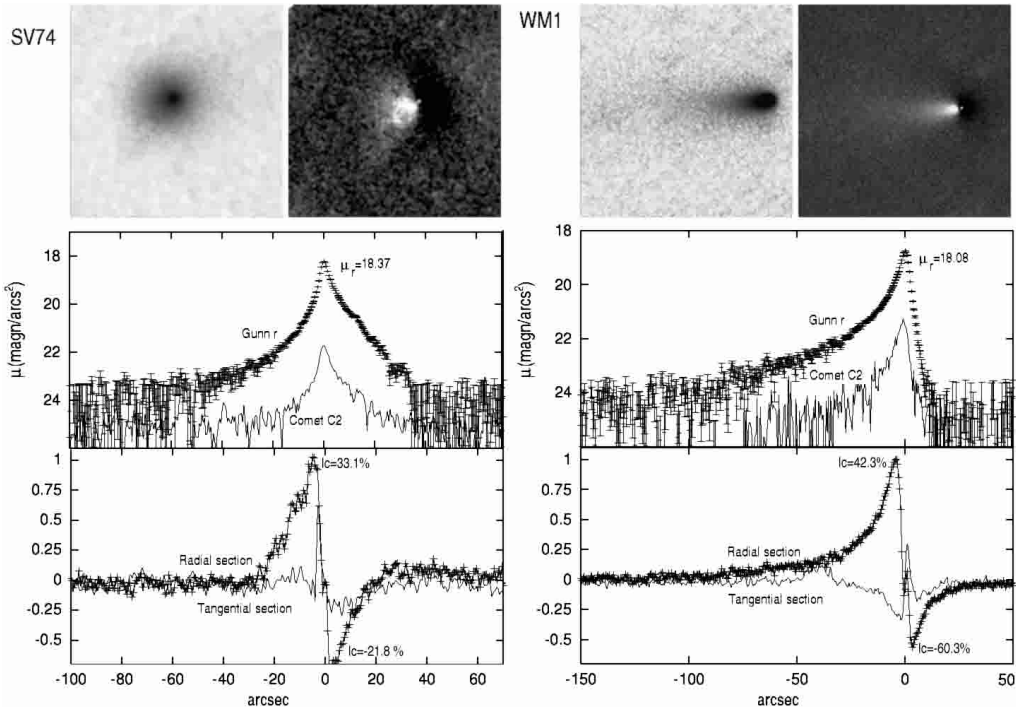

Fig. 2. continued. Comets C/2000 SV74 (left) and C/2000 WM1 (right). Size of images presented is $75'' \times 75''$ for C/2000 SV74 and $100'' \times 100''$ for C/2000 WM1.

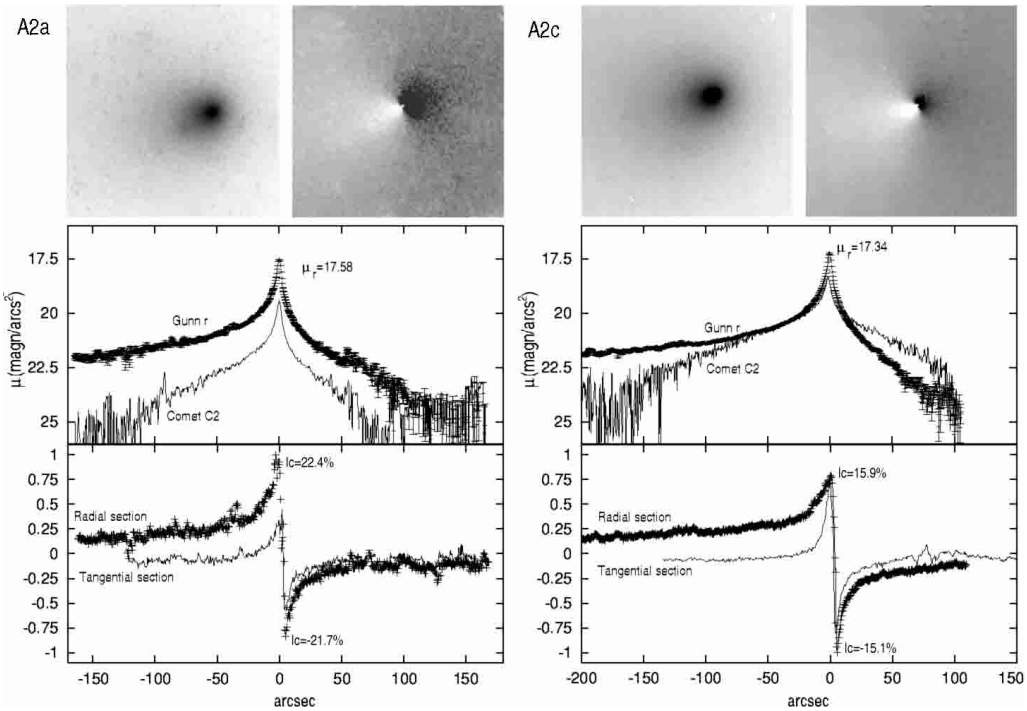

Fig. 2. continued. Comet C/2001 A2 on 13th (left) and 16th (right) August. Size of images presented is $150'' \times 150''$. Note the strong change of the C_2 profile.

We also detected a thin tail, brighter than 24 mag/arcsec^2 within $90''$ and decreasing to about 25 mag/arcsec^2 at $120''$ (corresponding to 260×10^3 km projected length) from the nucleus. Non-radial parts contribute 42% (maximum peak) and −60% (minimum peak), which we explain by radiation pressure on the coma. This is supported by the slope parameter of −1.42, which is common for comets at similar solar distance. The apparently long and thin tail directed exactly in the antisolar direction is evidence that the Sun has the greatest influence on the coma and tail shapes.

The level of activity seemed to be lower than in the case of C/2000 SV74 ($Af\rho$ = 275 cm): we measured relatively lower activity in C_2 and higher production of CO+. This is in good agreement with the canonical view of tail-formation, i.e. the dominant component of CO in cometary tails is observed at the examined wavelength (Arpigny 1995).

C/2001 A2 (LINEAR)

The comet was in the very focus of the scientific interest during the summer of 2001: as of September, 2001, there have been 25 IAU Circulars issued describing the evolution of this interesting comet. At the end of March, the comet brightened 4 magnitudes in 4 days (Mattiazzo et al. 2001). By the end of April, a double nucleus was detected (Hergenrother et al. 2001). Further fragmentation was reported by Schuetz et al. (2001), and a CN jet was reported by Woodney et al. (2001). At the second half of July, the comet diminished 3 magnitudes and rapid light variations were observed; these are explained by Kidger et al. (2001) as the separation of small, short-lived splinters that may not have been directly observable.

By the time of our observations, the total apparent magnitude decreased below eleventh magnitude, and none of the multiple nuclei was detectable on our images. Despite the "calm" behavior suggested by run A2a (on 13th August, 0:14 UT), a slight increase of activity was detected on A2b images (on 15th August, 0:00 UT). During the A2c run (on 16th August, 0:28 UT, production rates of CN and C_2 increased by a factor of 4, while dust production and $Af\rho$ did not vary much. The most surprising event between the nights is the variation of the shape of C_2 profile. The radiation pressure-dominated profile with narrow center turned into a quite extended, symmetric profile with little central hump. Some parts of the C_2 surface were brighter than the Gunn r continuum. That suggests a similar outburst of activity in C_2 and CN as was reported by many observers during the previous weeks (Kidger et al. 2001).

The Gunn r profile did not changed significantly between the two runs. In the central $7''$ the surface brightness falls by 2 magnitudes, while on the solar side it decreases by more than 5 magnitudes in about $70''$. On the antisolar side the coma evolves into an impressively bright and wide, V-shaped tail, which is brighter than 22 mag/arcsec^2 when it leaves the field of view As the tail character suggests merely dust components, the tail itself has also not been disturbed much by the observed small outburst. Altogether, the general morphology of C/2001 A2 is quite similar to the observed behavior of 19P/Borrelly. An important difference is that in the case of C/2001 A2, neither type of jet has been detected, and the azimuthally renormalized image shows a tail rich in dust and detectable until the nucleus.

Although the contribution of spatial variations parts slightly decreased during the outburst, the ratio of local contributions at minimum and maximum remained constant (i.e. 0.224/−0.217 vs. 0.159/−0.151) within an error of 4%. That may be explained by a spherically symmetric outburst. In this case, the absolute values of non-radial parts do not vary, but their contribution decreases as the absolute value of the radial part increases. Quantitatively, the radial part of the dust coma is increased by $39 \pm 2\%$. In this case, the brightness of the inner coma should increase $-0\overset{\mathrm{m}}{.}29$: that agrees with the observed value ($-0\overset{\mathrm{m}}{.}24$) within the expected errors.

A spherical outburst might be caused by uniformly increasing activity on the whole surface of the nucleus, though the little fractions of active area commonly observed in comets seem to contradict this view. Alternatively, matter ejected in fans above the active area can be blended to globular shape if we assume a fast-rotating nucleus. The assumption of a fast-rotating nucleus agrees with the observed break-up of small fractions of the nucleus.

The measured 162–191 cm $Af\rho$ is smaller than 288 cm measured by Schleicher (2001a), which is simply explained by the lower level of activity. Images and profiles are shown in Fig. 2c.

5. Discussion and concluding remarks

Five comets were observed few days before new moon in August, 2001. The comet producing the highest $Af\rho$ was 29P/Schwassmann–Wachmann 1 as it was caught during its outburst. Other comets also showed unusually high $Af\rho$ values, especially C/2000 SV74, which is predicted to become a fairly bright, dust-rich comet at perihelion.

Inner comae of comets often show more matter ejected to the solar side than elsewhere. This asymmetry of matter production is probably supported by the warm solar side of the nucleus. Comparing the continuum-dominated images and the emission-dominated ones, we find a significantly changing coma composition for C/2001 A2 in a smaller outburst. In the case of 19P and C/2001 A2, the solar side is dominated by gaseous components, due to interaction with the radiation pressure and solar wind: dusty components are blown backwards and the solar side becomes gas-rich. Outbursts, jets or proximity to the Sun may enrich gas in comae, and may lead to anomalous coma composition. We believe these factors explain the varying emission surface brightness profiles of C/2001 A2 in outburst.

In order to compare quantitatively the asymmetries in comets, the contributions of spatial variations are compared in Table 5. Peaks of maximal intensity are distinguished by their location relative to the center of the coma: s means peaks on the solar side, a denotes peaks on the anti-solar side. We classify peaks of minima as follows: r denotes radial-type peaks appearing near the radial section (solar or antisolar type), t denotes tangential-type peaks near the tangential section. The local contribution of spatial variations at minimum peaks seem to be well correlated with the geocentric radius. Similar but less obvious correlations can be found for the maxima, too. Generally, peaks of the azimuthally renormalized images

Table 5. Maxima and minima of spatial variations characterized as s solar and a antisolar, r radial or t tangential-type peaks. Distance from the nucleus is shown in 10^3 km.

Ref.	R(AU)	Δ(AU)	$D_{\max}$	$lc_{\max}$	$D_{\min}$	$lc_{\min}$
19P	1.400	1.685	5.5	0.342s	3.7	−0.398t
29P	5.919	5.121	26.1	0.370s	18.6	−0.769t
SV74	4.244	4.036	11.7	0.331a	5.9	−0.218rs
WM1	2.798	2.891	10.5	0.423a	7.3	−0.603rs
A2a	1.628	0.714	2.3	0.224a	1.3	−0.217rs
A2c	1.669	0.764	2.2	0.159a	1.4	−0.151rs

develop farther from the nucleus, and their contribution to the total coma intensity increases with increasing solar distance. This conclusion is consistent with the view that solar wind and radiation pressure affects the cold and slowly outflowing coma of less active comets at a larger solar distance.

C/2000 SV74 seems to be an exception to the rule, as its coma is significantly (by a factor of 3) less affected by spatial variations than the other four comets. This character can be hardly explained by the small phase angle or the generally circular appearance, and supports the idea that high level matter production is present that can challenge the solar wind.

Dependencies between Gunn-colors and $Af\rho$ parameter have been found for comets. Below we summarize the correlation, their standard errors (in brackets) and their regression coefficient. Independent correlations with better regression coefficient than 0.80 or −0.80 have been accepted.

$$\begin{aligned}(v-g) &= -0.51(20)+0.214(7)\cdot\log\, Af\rho[\mathrm{cm}]\\ &\quad \text{regr.coeff.}=0.87\\ (r-j) &= 0.12(5)+0.7(3)\cdot(v-g)\\ &\quad \text{regr.coeff.}=0.81\\ (j-z) &= 0.19(4)-0.8(2)\cdot(r-j)\\ &\quad \text{regr.coeff.}=-0.88.\end{aligned}$$

We explain the correlation between $v-g$ color and $Af\rho$ as a scattering effect of dust. Matter particles scatter the short-wavelength violet color the most, thus, the more dust present in the coma, the more "reddish" $(v-g)$ its color. Continuum colors of 29P/Schwassmann-Wachmann 1 are measured to be slightly less reddish than previously published values: $B-V=0.8$ (Hartmann et al. 1982), $V-R=0.502$ and $R-I=0.492$ (Meech et al. 1993), which may be transformed into the Gunn-system with help of the transformations determined by Kent (1985) and Jørgensen (1996), yielding $v-g=0.478$, $g-r=0\overset{\mathrm{m}}{.}028$. Meech et al. (1993) attribute reddish colors to a large distance from the Sun. In present paper, the experimental correlation between $Af\rho$ and $(v-g)$ also explains quite reddish colors.

Correlation between $r-j$ and $j-z$ may be an artificial effect. Examining the individual comets, the $j-z$ color is found to correlate with solar distance as the radiation contribution in the near-infrared has increasing effect with decreasing solar distance.

In order to understand production rates, we have compared our data to the extensive set of A95. In the case of 19P/Borrelly, production rate ratios are in a perfect agreement with the previous results, as mentioned in A95. The detected lance-head shape of the coma is similar to the HST images taken by Lamy et al. (1998). Their slope parameter varying around −1 with moderate angular variations is in a perfect agreement with our observations. We note that Schleicher (2001b) published $Af\rho$ measurements in September, which were half those measured by us. The slope parameter $G=-1.9$ of Schleicher (2001b) is also not comparable with our smooth profile.

C/2000 SV74 and C/2000 WM1 have similar appearances, although during their further evolution significant structural differences may develop, due to the difference in their perihelion distances (3.54 and 0.56 AU). The abundance of C_2 in C/2000 SV74 is much higher than usual: one can find only 3 comets (P/Russel 4, C/Shoemaker 1984 XII, C/Shoemaker 1984 XV) with higher C_2/CN production among the 85 objects discussed in A95.

C/2001 A2 showed a significant change in composition during its outburst. Compared to the statistics and Fig. 4c of A95, the $[Af\rho]$–[CN] seems to be anomalously high in "quiescent" state (−22.07), while is also a bit high, but not peculiar, in "outburst" (−22.74); these values fall within the -23.1 ± 0.9 interval for all of the comets discussed in A95. As a possible explanation, one can imagine that C/2001 A2 was in a period of anomalously low activity, a "negative outburst", during the time of high $[Af\rho]$–[CN] production (e.g. A2a, on 13th August, 0:14 UT). The normal behaviour in outburst-like events is to show increased gas activity.

Comets 19P and C/2001 A2 show similarly bluish colors and CN-rich gas production. Low $[C_2]$–[CN] rates allow us to classify C/2001 A2 as a Borrelly-type comet (Fink et al. 1999). Note that the drastic variations observed during some months previously might also influence the classification.

Finally, we summarize our results as follows.

1. The use of Gunn photometric system in structural and production analysis of comets is demonstrated. When augmented with comet and continuum interference filters, the system combines the advantages of the two systems usually preferred in cometary astronomy (Johnson filters for morphology and narrow-band filters for spectrophotometric studies).
2. A technique for generating and analyzing azimuthally renormalized images or non-radial residual maps is discussed, and the power of this tool to study morphology is demonstrated. In the case of C/2000 SV74, C/2000 WM1 and C/2001 A2, simple comae with slight solar formation effects are observed. In the case of 19P/Borrelly, slope parameter was almost −1, but spatial variations were observed to make moderate contributions. 29P/Schwassmann-Wachmann 1 was observed in outburst, and a well-developed jet and a ring at larger

nuclear distance were detected. Variations from spherical outflow are indicated by local contribution parameters at the peaks of the azimuthally renormalized images. Generally, the contribution of the non-radial parts to the whole coma was found to increase with the solar distance. 3. C/2000 SV74 and C/2000 WM1 were observed a few months before their perihelion. Large $Af\rho$ values, the extended coma of C/2000 SV74 and the nice tail of C/2000 WM1 suggest that they will be interesting objects in perihelion. C/2000 SV74 showed unusually high [C_2]–[CN] production ratio, and developed a nearly spherical coma at a distance of 4 AU. During our observations, C/2001 A2 suffered a smaller outburst, ejecting mainly gaseous components. The ejected matter evolved in a spherically symmetric manner. The amount of gas increased by a factor of 4 during the outburst, while the dust components increased by about 39%. Its matter production is quite atypical when low level of activity is present.

Acknowledgements. This research was supported by FKFP Grant 0010/2001, Pro Renovanda Cultura Hungariae Grant DT 2001. május/21., OTKA Grants #T032258 and #T034615, "Bolyai János" Research Scholarship of LLK from the Hungarian Academy of Sciences, "Koch Sándor" Foundation (Ref. number KSA 2001/8) and Szeged Observatory Foundation. The warm hospitality and helpful assistance of the staff of Calar Alto Observatory is gratefully acknowledged. The authors also acknowledge suggestions and careful reading of the manuscript by Dr. Michael Richmond. The NASA ADS Abstract Service was used to access data and references.

References

A'Hearn, M. F. 1983, in Solar System Photometry, ed. R. Genet (Willmon Bell, Virginia)
A'Hearn, M. F., Millis, R. L., Schleicher, D. G., et al. 1995, Icarus, 118, 223 (A95)
Alekseeva, G. A., Arkharov, A. A., Galkin, V. D., et al. 1996, Baltic Astr., 5, 603
Arpigny, C. 1995, ASP Conf. Ser., 81, 362
Enzian, A., Cabot, H., & Klinger, J. 1997, A&A, 319, 995
Fink, U., & Hicks, M. D. 1996, ApJ, 459, 729
Fink, U., Hicks, M. P., & Fevig, R. A. 1999, Icarus, 141, 331
Gaffey, M. J., Burbine, T. H., & Binzel, R. P. 1993, Meteoritics, 28, 161
Hartmann, W. K., Cruikshank, D. P., & Degewij, J. 1982, Icarus, 52, 337
Hergenrother, C. W., Chamberlain, M., Chamberlain, Y., et al. 2001, IAUC, 7616
Jørgensen, I. 1996, PASP, 106, 967
Jewitt, D. 1990, ApJ, 351, 277
Kent, S. M. 1985, PASP, 97, 165
Kidger, M., Ferrando, R., Manteca P., et al. 2001, IAUC, 7679
Lamy, P. L., & Tóth, I. 1995, A&A, 293, L43
Lamy, P. L., Tóth, I., & Weaver, H. A. 1998, A&A, 337, 945
Larson, S. M., & Slaughter, C. D. 1992, Asteroids, Comets, Meteors 1991, 337–343
Lederer, S., Campins, H., & Osip, D. J. 1997, EMP, 78, 131
Lowry, S. C., Fitzsimmons, A., Cartwright, I. M., & Williams, I. P. 1999, A&A, 349, 649
Luu, J. X., & Jewitt, D. C. 1992, AJ, 104, 2243
Mattiazzo, M., et al. 2001, IAUC, 7605
Meech, K. J., Belton, M. J. S., & Mueller, B. E. A. 1993, AJ, 106, 1222
Nakamura, A., Hale, A., Kadota, K., & Yoshimoto, K. 2001, IAUC, 7640
Ravindranath, S., Ho, L. C., Peng, C. Y., et al. 2001, AJ, 122, 653
Schleicher, D. 2001a, IAUC, 7653
Schleicher, D. 2001b, IAUC, 7722, 2–3
Schuetz, O., Jehin, E., Bonfils, X., et al. 2001, IAUC, 7656
Schultz, R., A'Hearn, M. F., Birch, P. V., et al. 1993, Icarus, 104, 206
Szabó, Gy., Csák, B., Sárneczky, K., & Kiss, L. L. 2001, A&A, 374, 712
Thuan, T. X., & Gunn, J. E. 1976, PASP, 88, 543
Woodney, L. M., Schleicher, D. G., & Greer, R. 2001, IAUC, 7666
Wade, R. A., Hoessel, J. G., Elias, J. H., & Huchra, J. P. 1979, PASP, 91, 35